

# NMR analysis of the backbone dynamics of the small GTPase Rheb and its interaction with the regulatory protein FKBP38

Maristella De Cicco<sup>1</sup>, Leo Kiss<sup>1,\*</sup> and Sonja A. Dames<sup>1,2</sup>

<sup>1</sup> Technische Universität München, Department of Chemistry, Biomolecular NMR Spectroscopy, Garching, Germany

<sup>2</sup> Institute of Structural Biology, Helmholtz Zentrum München, Neuherberg, Germany

## Correspondence

S. A. Dames, Department of Chemistry,  
Biomolecular NMR Spectroscopy,  
Lichtenbergstr. 4, 85747 Garching, Germany  
Fax: +49-(0)89-28913869  
Tel: +49-(0)89-28913292  
E-mail: sonja.dames@tum.de

## \*Present address

Institute of Pharmacy and Molecular  
Biotechnology, Universität Heidelberg,  
69120 Heidelberg, Germany

(Received 3 May 2017, revised 6 October  
2017, accepted 17 November 2017)

doi:10.1002/1873-3468.12925

Edited by Christian Griesinger

Ras homolog enriched in brain (Rheb) is a small GTPase that regulates mammalian/mechanistic target of rapamycin complex 1 (mTORC1) and, thereby, cell growth and metabolism. Here we show that cycling between the inactive GDP- and the active GTP-bound state modulates the backbone dynamics of a C-terminal truncated form, Rheb $\Delta$ CT, which is suggested to influence its interactions. We further investigated the interactions between Rheb $\Delta$ CT and the proposed Rheb-binding domain of the regulatory protein FKBP38. The observed weak interactions with the GTP-analogue-(GppNHp-) but not the GDP-bound state, appear to accelerate the GDP to GTP exchange, but only very weakly compared to a genuine GEF. Thus, FKBP38 is most likely not a GEF but a Rheb effector that may function in membrane targeting of Rheb.

**Keywords:** backbone dynamics; FKBP38; GTPase; nucleotide exchange rate; protein–protein interactions; Rheb

Human Ras homolog enriched in brain (Rheb) is a small guanosine triphosphatase (GTPase) and accordingly shuttles between an inactive GDP- and an active GTP-bound state (Fig. 1A). The G1–G5 boxes (GDP/GTP-binding motifs) that partially overlap with three motifs known as phosphate-binding loop (P-loop) and switch 1 and 2 are conserved in GTPases and can also be found in human Rheb (Fig. 1B). These regions mediate nucleotide-binding and/or sensing of the type of bound nucleotide and/or are involved in GTP hydrolysis as well as its regulation [1–3]. Rheb adopts a typical GTPase fold consisting of a mixed six-stranded beta sheet with five helices packing around it

[4,5]. During GDP to GTP cycling, the switch 1 region of Rheb undergoes a conformational change while the switch 2 region maintains a stable, extended conformation that differs significantly from the  $\alpha$ -helical conformation seen in other small GTPases and that results in an orientation of Q64, which is equivalent to the catalytic Q61 of Ras, that disables GTP hydrolysis thereby explaining its low intrinsic GTPase activity [4].

Rheb is a well-known regulator of the mammalian/mechanistic target of rapamycin (mTOR), a master controller of cell growth and metabolism in response to the availability of nutrients and growth factors [6–10]. mTOR is found in two functionally and

## Abbreviations

FKBP38, FK506-binding protein of 38 kDa (also known as FKBP-8); GAP, GTPase-activating protein; GDP, guanosine diphosphate; GEF, guanine nucleotide exchange factor; GppCp (also known as GMPPCP and GppCH<sub>2</sub>p), guanosine-5'-[( $\beta$ , $\gamma$ )-methylene]triphosphate, sodium salt; GppNHp (also known as GMPPNP), guanosine-5'-[( $\beta$ , $\gamma$ )-imidio]triphosphate, trisodium salt; mTOR, mammalian/mechanistic target of rapamycin; Rheb, ras homolog enriched in brain.

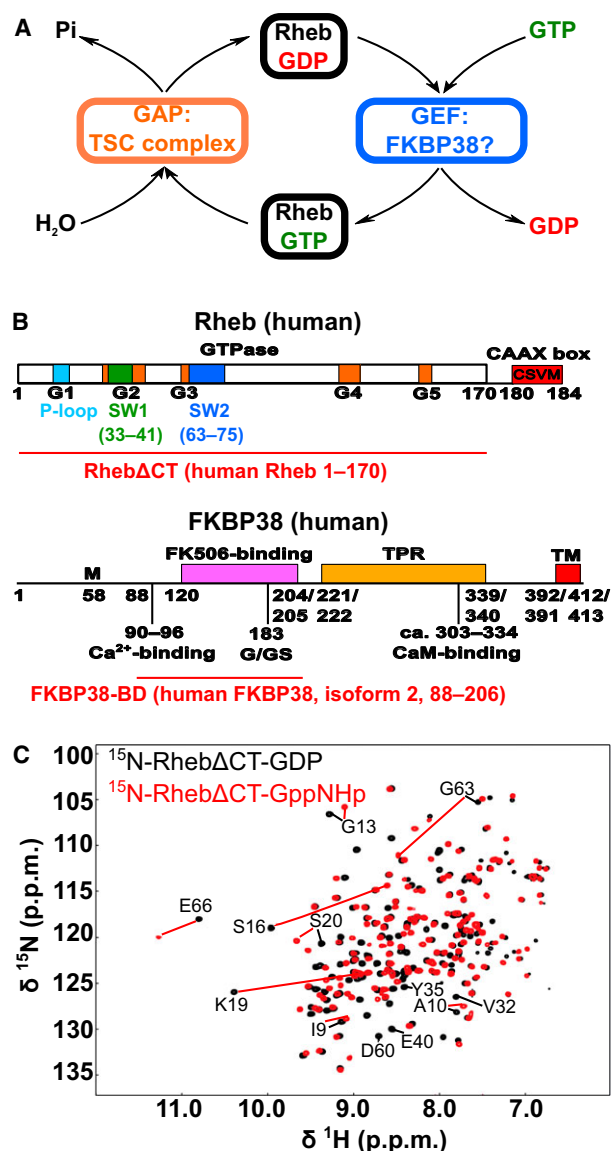


**Fig. 1.** The small GTPase Rheb switches between an active GTP- and an inactive GDP-bound state and has been suggested to be regulated by the FKBP12-related protein FKBP38. (A) The activation and deactivation cycle of Rheb. The TSC complex acts as a GTPase-activating protein (GAP) for Rheb. It has not been analyzed if FKBP38 has some guanine nucleotide exchange factor (GEF)-like activity on Rheb. (B) Domain structures of human Rheb and human FKBP38. The G boxes and the two switch regions (SW1 and SW2) are indicated [1,3]. The cysteine in the C-terminal CAAX box is post-translationally farnesylated. The C-terminally truncated fragment (1–170) used within this study is referred to as Rheb $\Delta$ CT. Human FKBP38 exists in two isoforms and has different functional regions (TPR, tetratricopeptide repeat domain; TM, transmembrane domain). For this study, residues 88–206 of isoform 2 that has GS instead of only G at position 183 encompassing the binding region for Rheb [62] and referred to as FKBP38-BD was used. (C) Superposition of the  $^1\text{H}$ - $^{15}\text{N}$  HSQC spectra of  $^{15}\text{N}$ -Rheb $\Delta$ CT in the GDP- (black) and GTP analogue- (= GppNHp, red) bound form. Several residues showing large chemical shift changes between the two states are labeled with the one letter amino acid code and the residue sequence position and in the same color as used for the respective spectrum. The fully assigned spectra for each state as well as that of Rheb $\Delta$ CT bound to another GTP analogue, referred to as GppCp, are displayed in Fig. S1-S3, respectively. Fig. S3 shows further a superposition of the  $^1\text{H}$ - $^{15}\text{N}$  HSQC spectra of  $^{15}\text{N}$ -Rheb $\Delta$ CT in the GppNHp- and GppCp-bound states.

structurally distinct heteromeric complexes, named mTOR complex 1 and 2 (mTORC1 and mTORC2) [11,12]. Rheb in the active GTP-bound state is an mTORC1 activator [13]. The Rheb mutants D60V and D60K are unable to bind GTP or GDP [14,15]. Based on co-immunoprecipitation assays using wild-type or mutant Rheb expressed in HEK293 cells, the D60V and D60K mutants could also interact with mTOR complexes, which suggested that the interaction does not depend on the nucleotide-binding state [16]. The tuberous sclerosis complex protein complex is composed of the proteins tuberous sclerosis complexes 1 and 2 (TSC1 and TSC2 also known as hamartin and tuberin, respectively) as well as Tre2-Bub2-Cdc16-1 domain family member 7 (TBC1D7) [17–19]. TSC2

functions as GTPase-activating protein (GAP) for Rheb that promotes GTP hydrolysis thereby inactivating Rheb and thus inhibiting mTORC1 signaling [15,20–22]. Rheb and TSC2 are a special GTPase-GAP pair since the first has a high basal GTP-state level and the latter uses instead of the catalytic arginine finger found in the Ras-GAP an asparagine thumb [15]. Based on the crystal structure of Rheb bound to GTP, shielding of the phosphate moiety by the conserved Y35 of switch 1 appears to disable the insertion of an arginine finger [4]. The role of translationally controlled tumor protein (TCTP) as guanine nucleotide exchange factor [23] has been questioned [24] and other GEFs have yet not been detected.

Rheb and Rheb-like protein 1 (RhebL1), which play a similar role for TOR signaling [25], have both a C-terminal CAAX (C = cysteine, A = aliphatic, X = terminal amino acid) box (Fig. 1B) that becomes post-translationally farnesylated resulting in targeting to endomembranes, primarily to the ER and the Golgi apparatus [26,27]. Failure of Rheb to localize to endomembranes impairs the interaction with mTOR [26]. TOR has been localized at different cellular membrane compartments and in the nucleus, which has recently been reviewed [28]. In response to amino acids, the so-called Rag and Ragulator complexes mediate the translocation of mTORC1 to the outer lysosomal membrane, to which also Rheb can localize

[29,30]. It has been suggested that Rheb is activated at the Golgi apparatus and then translocates to the lysosome and that this is connected to the maturation of endosomes to lysosomes [31].

FKBP38, a member of the FKBP506-binding protein family, has been suggested to function as an endogenous inhibitor of mTORC1 activity, whose action is antagonized by Rheb and RhebL1 in response to growth factor stimulation and good nutrient availability [32,33]. Human FKBP38 contains different functional regions and different isoforms exist and are further obtained by alternative splicing (Fig. 1B). The N-terminal glutamate-rich region is followed by a FKBP12-like prolyl isomerase (PPIase) domain, referred to as FKBP-C. The structure of the FKBP-C domain and its interaction with FK506 and Bcl-2 have been characterized [34–38]. Binding of calcium-saturated calmodulin (CaM) to its further C-terminal recognition site activates the constitutively inactive PPIase and enables the interaction with Bcl-2 [39,40]. A low-affinity cation-binding site in the FKBP-C region may further regulate the interaction with Bcl-2 in response to calcium ion levels [35]. The C-terminal transmembrane domain mediates localization to the outer membranes of the ER and mitochondria [41–44]. Based on GST pull-down assays, the FKBP-C domain of FKBP38 interacts with the same region of human TOR (residues 1967–2191) that had been suggested to interact with Rheb [13,32]. However, Bai *et al.* could not verify the latter interaction but instead suggested that Rheb interacts with the FKBP-C domain of FKBP38 in a GTP-dependent manner [32]. The not necessarily direct interaction between FKBP38 and Rheb-GTP but also Rheb-GDP had been confirmed by Wang *et al.*, but they were unable to confirm an influence of amino acid or insulin treatment on the FKBP38-mTOR interaction [45]. The interaction between Rheb and FKBP38 was further examined in detail based on three different *in vitro* assays, but could not be verified with any of them [46]. Thus, questions about the TOR-Rheb-FKBP38 interaction network remain and further studies are necessary to resolve if the interactions are direct or not and if they only occur under specific conditions.

In order to resolve the described conflicting results regarding the role of FKBP38 for the regulation of the GTPase Rheb, we conducted the following NMR studies. Since dynamic regions often play an important role for interactions with regulatory proteins, we first characterized the backbone dynamics of human Rheb lacking the CAAX box (residues 1–170 = Rheb $\Delta$ CT) in the inactive GDP and the active-like GTP analogue-bound state based on  $^{15}\text{N}$ -relaxation data. In addition,

we monitored the interaction with FKBP38 in both nucleotide-binding states and analyzed if FKBP38 might influence the backbone dynamics of the GTP analogue-bound state or stimulate the exchange of GDP to GTP and thus show some kind of guanine nucleotide exchange factor (GEF)-like activity.

## Materials and methods

### Protein expression and purification

All used proteins were expressed in *Escherichia coli* (*E. coli*) BL21 (DE3) cells (Novagen).  $^{15}\text{N}$  and  $^{13}\text{C}$  labeling was carried out by growth in minimal medium (M9) containing  $^{15}\text{NH}_4\text{Cl}$  and  $^{13}\text{C}_6$ -glucose as sole nitrogen and carbon sources, respectively.

A C-terminal truncated version of human Rheb (Uniprot-ID Q15382) lacking the CAAX box needed for farnesylation (1–170 = Rheb $\Delta$ CT) was expressed as a glutathione-S-transferase (GST) fusion protein from pGEX-4T. When the OD<sub>600</sub> of the culture that had been grown at 37 °C was around 0.6–0.8, cells were induced with 0.1 mM isopropyl-B-D-thiogalactopyranoside at 15 °C overnight. Cells were disrupted in 50 mL 20 mM Tris, 100 mM NaCl, 5 mM MgCl<sub>2</sub>, and 2 mM benzamidine, pH 7.5, by sonication (Sonoplus Bandelin, UV 3200) for 15 min on ice with a power level of 35% and a pulse length of 5 s. Following centrifugation, the supernatant was loaded on a Glutathione Sepharose<sup>®</sup> 4B (GE Healthcare) column and the target protein purified according to the manufacturer's manual, except for the fact that the used buffers contained no Triton X-100. Following adjustment of the eluate pH to 7.5, the GST tag was cleaved off by adding thrombin (Serva, 5 U per mg fusion protein) and incubation at room temperature over night on a slowly rocking device. Thrombin cleaves between the R and the G of its recognition sequence (LVPR<sup>^</sup>GS) thereby leaving two non-native residues (GS) at the N terminus. Rheb $\Delta$ CT was separated from the GST tag by size exclusion chromatography using a 75  $\mu\text{g}$  Superdex<sup>™</sup> HiLoad<sup>™</sup> 16/600 column (GE Healthcare) coupled to an ÄKTA Prime FPLC system (GE Healthcare) and equilibrated in 20 mM Tris, 150 mM NaCl, 5 mM MgCl<sub>2</sub>, pH 7.5. The used flow rate was 1 mL·min<sup>-1</sup>. Eluted fractions that contained based on an SDS/PAGE analysis Rheb $\Delta$ CT were pooled and concentrated using centrifugal filter devices (Amicon<sup>®</sup> Ultra Centrifugal Filter Units MWCO 3000, 15 mL, Merck Millipore) at 3500 g and 4 °C.

FKBP38-BD (Uniprot-ID 14318, residues 88–206 of human FKBP38 isoform 2, Fig. 1B) was expressed as His-tagged protein from a pET-16b (Novagen) expression vector. When the OD<sub>600</sub> of the culture that had been grown at 37 °C was around 0.8, cells were induced with 0.5 mM IPTG at 37 °C overnight. The by centrifugation harvested cells from 1 L culture were resuspended in 50 mL 50 mM

Tris, 2 mM EDTA, 2 mM benzamidine, 2 mM DTT, pH 8, and lysed by sonication as described for Rheb $\Delta$ CT. Since most of the protein expressed in inclusion bodies, the pellet obtained after another centrifugation step was washed with 20 mL 50 mM Tris, 1 M urea, 1 mM TCEP, pH 8. Extraction of the His-tagged FKBP38-BD from the inclusion body pellet was done by adding 15 mL 50 mM Tris, 6 M guanidinium chloride (GdmCl), 1 mM TCEP, pH 8, manual disruption of the pellet, and incubation on a rocking device for 1 h at 4 °C. Following centrifugation at 23 000 *g* at 4 °C for 30 min, the supernatant was loaded on a Ni-NTA resin (Qiagen) filled column (5 mL) that had been equilibrated in 50 mM Tris, 6 M GdmCl, 1 mM TCEP, 30 mM imidazole, pH 8. The protein bound to the column was refolded by step-wise decreasing the concentration of GdmCl from 6 to 0 M in 1 M steps. The refolded protein was eluted with 40 mL 50 mM Tris, 350 mM NaCl, 1 mM TCEP, 500 mM imidazole, pH 8. Eluted fractions that contained based on an SDS/PAGE analysis the target protein were pooled and concentrated to 2.5 mL using centrifugal filter devices (Amicon<sup>®</sup> Ultra Centrifugal Filter Units MWCO 3000, 15 mL, Merck Millipore) at 3500 *g* and 4 °C. Following exchange of the buffer to 20 mM Tris, 100 mM NaCl, 1 mM CaCl<sub>2</sub>, pH 8, using a PD-10 column (GE Healthcare), factor Xa (New England Biolabs, 1 U per 50  $\mu$ g substrate protein) was added to cleave off the His-tag at 25 °C overnight. FKBP38-BD was separated from the His-tag by size exclusion chromatography and pooled and concentrated as described for Rheb $\Delta$ CT.

A 13mer peptide corresponding to the switch1 region of human Rheb (residues 33–45 referred to as hRheb\_sw1 = Acetyl-NH-DSYDPTIENTFTK-CONH<sub>2</sub>) was bought from Thermo Scientific. A stock solution for the NMR monitored titration with <sup>15</sup>N-FKBP38-BD was obtained by dissolving 2.2 mg lyophilized peptide in 0.9 mL 20 mM Tris, 150 mM NaCl, 5 mM MgCl<sub>2</sub>, pH 7.5.

### Sample preparation for the NMR studies

Samples contained 80–200  $\mu$ M Rheb $\Delta$ CT for the NMR-monitored interaction studies and 310–380  $\mu$ M protein to record 3D HNCA and 3D CCONH-TOCSY, and <sup>15</sup>N-relaxation data in 20 mM Tris, 150 mM NaCl, 5 mM MgCl<sub>2</sub>, pH 7.5 supplemented with 5% D<sub>2</sub>O. From *E. coli* cells, the GDP-bound form is primarily purified. The GTP analogue- (guanosine 5'-[ $\beta,\gamma$ -imido]triphosphate, trisodium salt = GppNHp, also known as GMPPNP, and guanosine-5'-[( $\beta,\gamma$ -methylene]triphosphate, sodium salt = GppCp-, also known as GMPPCP and GppCH<sub>2</sub>p, used as 50 mM stocks in buffer, Jena Bioscience) bound forms were obtained by adding a 10-fold excess of the respective nucleotide to the GDP form in 20 mM Tris, 150 mM NaCl, 5 mM MgCl<sub>2</sub>, pH 7.5, in the presence of 10 mM EDTA to decrease the affinity for GDP [47–49] and a catalytic amount of Antarctic phosphatase

(5 U = 1  $\mu$ L for each NMR sample of 0.25 mL, New England Biolabs) to degrade GDP [49–51]. To record 3D assignment and <sup>15</sup>N-relaxation data, the samples were incubated for 7 days at 4 °C to achieve a complete exchange from the GDP to the GppNHp or the GppCp form.

All the samples used to determine the influence of FKBP38-BD on the GDP to GppNHp exchange rates (see also Table 1) contained about 0.1 mM <sup>15</sup>N-Rheb $\Delta$ CT-GDP in the usual buffer supplemented with 0.5 mM GppNHp, 1 (series A–C) or 10 (series F–H) mM EDTA, 5 units Antarctic phosphatase (= PPase, New England Biolabs, 1  $\mu$ L with 5000 units·mL<sup>-1</sup> for each 0.25 mL sample) in the first and second subseries (A1 to H1 and A2 to H2), and either no FKBP38-BD in the first subseries of each series (A1 to H1) or at the following molar ratios of <sup>15</sup>N-Rheb $\Delta$ CT-GDP to FKBP38-BD: 102 : 1 (A2/3-C2/3), or 96 : 1 (F2/3) or 29 : 1 (G2/3) or 15 : 1 (H2/3). It should be noted that the use of EDTA alone or together with phosphatase does not correspond to physiological conditions; however, it allows to modulate the time scale of the reaction to make it suitable for the used detection method and has been described in several studies of GTPases [47–52]. The effect of the used EDTA concentrations on the Mg<sup>2+</sup> concentration should be rather low since the affinity of EDTA for Mg<sup>2+</sup> is much lower than for other divalent metal ions such as for example Zn<sup>2+</sup> [53]. Antarctic phosphatase needs Zn<sup>2+</sup> (and also Mg<sup>2+</sup>) ions for its activity (New England Biolabs data sheet). Because of this, its activity in the presence of EDTA is expected to be reduced. The effect of EDTA on the activity has been analyzed for alkaline phosphatases from different tissues. Whereas bone and intestinal phosphatases display an increasing loss in activity with increasing concentrations of EDTA, placental phosphatase displays a progressive gain in activity with increasing concentration of EDTA [54]. Because the combined use of EDTA and phosphatase (in this case calf intestine alkaline phosphatase) had been described for the sample preparation of Rheb bound to a GTP analogue [49], we also tried this buffer condition to monitor the effect of FKBP38-BD on the GDP to GppNHp exchange in addition to the use of only EDTA to promote the formation of the GTP analogue-bound state ([47,48], Table 1).

### NMR spectroscopy

NMR spectra were acquired at 298 K on Bruker Avance 500 and 600 MHz spectrometers, the 500 MHz and one of the 600 MHz spectrometers equipped with a cryogenic probe. Data were processed with NMRPipe [55] and analyzed using NMRView [56]. Chemical shift assignments for rat and mouse Rheb in the GDP- and/or GppNHp-bound forms have been published [49,57,58]. Since we used human Rheb and a slightly different fragment and/or buffer conditions, we assigned the backbone <sup>1</sup>H, <sup>15</sup>N, and <sup>13</sup>C $\alpha$  nuclei based on newly recorded 3D HNCA and CCONH-TOCSY

**Table 1.** Overview of the analysis of the GDP to GppNHp exchange of Rheb $\Delta$ CT in the absence and presence of FKBP38-BD and/or Antarctic phosphatase (= PPase) by real-time NMR spectroscopy.

Series name	[Rheb $\Delta$ CT]: [FKBP38-BD] <sup>a</sup>	Addition of PPase	[EDTA] (mM)	Analyzed residues	Average exchange time $\tau_{ex}$ (min) $\pm$ standard deviation <sup>b</sup>
A1	1 : 0	Yes	1	A10, G13, K19, S20, V32,	132 $\pm$ 55
A2	102 : 1	Yes	1	Y35, E40, D60, G63, Q64	297 $\pm$ 77
A3	102 : 1	No	1		52 $\pm$ 30
B1	1 : 0	Yes	1	I9, A10, G13, S20, V32, Y35, E40, G63	128 $\pm$ 35
B2	102 : 1	Yes	1		163 $\pm$ 62
B3	102 : 1	No	1		133 $\pm$ 46
C1	1 : 0	Yes	1	A10, S20, Y35, E40, D60, G63, Q64	329 $\pm$ 108
C2	102 : 1	Yes	1		239 $\pm$ 108
C3	102 : 1	No	1		267 $\pm$ 120
F1	1 : 0	Yes	10	I9, A10, G13, S16, K19, S20, V32,	108 $\pm$ 19
F2	96 : 1	Yes	10	Y35, E40, D60, G63, Q64, E66	101 $\pm$ 17
F3	96 : 1	No	10		74 $\pm$ 38
G2	29 : 1	Yes	10	None, because of too fast exchange	–
G3	29 : 1	No	10		–
H2	15 : 1	Yes	10		–
H3	15 : 1	No	10		–

<sup>a</sup>The Rheb $\Delta$ CT concentration in the samples was always  $\approx$  100  $\mu$ M (A series: 98, B series: 114, C series: 106  $\mu$ M). The concentration of GppNHp was always 0.5 mM.

<sup>b</sup>The average was taken over all residues analyzed for a particular series (see column labeled 'analyzed residues').

data in combination with the published assignments. The  $^1\text{H}$  and  $^{15}\text{N}$  resonances of Rheb-GppCp were assigned based on the similarity of its  $^1\text{H}$ - $^{15}\text{N}$  HSQC spectrum to that of Rheb-GppNHp. The assigned  $^1\text{H}$ - $^{15}\text{N}$  HSQC spectra for Rheb $\Delta$ CT-GDP, Rheb $\Delta$ CT-GppNHp, and Rheb $\Delta$ CT-GppCp are displayed in Figs S1–S3, respectively.

Information about the backbone dynamics was derived from the measurement of  $^{15}\text{N}$ -relaxation experiments, including  $T_1$ ,  $T_2$ , and  $\{^1\text{H}\}$ - $^{15}\text{N}$  NOE. The relaxation times were sampled at the following time points: for  $T_1$ : 10.8, 216, 432, 648, 864 ms; for  $T_2$ : 25.6, 51.2, 76.8, 102.4, 128 ms. Relaxation times were determined based on a fit to the equation  $y = A \exp(-t/B)$ , where B corresponds to  $T_1$  or  $T_2$  and A to the signal intensity at time 0, using the relaxation analysis tool provided in NMRView.  $^{15}\text{N}$ - $T_1$ ,  $^{15}\text{N}$ - $T_2$ , and  $\{^1\text{H}\}$ - $^{15}\text{N}$ -NOE values of well-resolved peaks of different nucleotide-binding states of Rheb $\Delta$ CT were analyzed based on a model-free approach [59,60] using the program TENSOR2 [61] and the solution structure of rat Rheb-GDP (PDB-ID 2L0X) and the crystal structure of mouse Rheb-GppNHp (PDB ID 4O25). For the determination of the rotational correlation time,  $\tau_c$ , residues for which  $T_1/T_2$  was within one standard deviation from the average value were considered (for Rheb $\Delta$ CT-GDP: 6–12, 14–16, 18–22, 24–29, 31–36, 38–48, 51–66, 68, 69, 74–79, 83–99, 105–112, 118–125, 127–152, 154–161, 163–170; for Rheb $\Delta$ CT-GppNHp: 6–14, 16–18, 20–23, 26–29, 43–49, 51–59, 63, 65–68, 77, 79–88, 90, 92–102, 107–112, 114–124, 126–152, 154–160, 162, 164–170).

To monitor the exchange times of bound GDP to GppNHp in  $^{15}\text{N}$ -Rheb $\Delta$ CT in the absence and presence of FKBP38-BD and/or Antarctic phosphatase (= PPase) by NMR (Table 1), the samples were brought to the NMR machine right after mixing. The times given in the spectra pictures (Fig. 4A,C,D, Figs S8–S9, S10A,B) refer to the time the respective  $^1\text{H}$ - $^{15}\text{N}$  HSQC experiment was started after mixing of the sample. To determine the exchange times, only backbone amide resonances for residues sensitive to the nucleotide exchange and thus showing a significant change in the  $^1\text{H}$  and  $^{15}\text{N}$  chemical shifts between the GDP- and the GppNHp-bound states were analyzed (Fig. 1C). Usually, I9, A10, S16, K19, S20, V32, Y35, E40, G63, Q64, and E66 were considered. Exchange times ( $\tau_{ex} = 1/k_{ex}$ ) were obtained by fitting the signal intensity for the recorded time points to an exponential decay function ( $y = A \exp(-t/B) + C$ , where B corresponds to  $\tau_{ex}$  and A to the signal intensity in the  $^1\text{H}$ - $^{15}\text{N}$  HSQC spectrum corresponding to the first time point, and C to the offset along the y-axis), using the rate analysis tool provided in NMRView. In some series the error of the fitted exchange times were very high (> 30 min) because of too low signal intensity in most of the spectra of the respective time series. Accordingly, the corresponding values were not used to calculate average exchange times ( $\tau_{ex}(\text{average})$ , Table 1). As a control, we looked at the  $^1\text{H}$ - $^{15}\text{N}$  peak intensity of I90, which is not affected by the GDP to GppNHp exchange and which thus should not show an exponential decay of its signal intensity.

## Results

### The inactive GDP- and the active-like GppNHp-bound states of C-terminally truncated Rheb show differences in the backbone dynamics in GTPase-specific regulatory regions

In line with published crystal structure data [4], the superposition of the  $^1\text{H}$ - $^{15}\text{N}$  HSQC spectra of Rheb $\Delta\text{CT}$ -GDP and Rheb $\Delta\text{CT}$ -GppNHp (Fig. 1C) indicates that GDP to GTP cycling results in significant conformational changes. In order to determine if the inactive GDP- and the active GTP-bound state of

Rheb show differences in the backbone dynamics that may play a functional role, we analyzed  $^{15}\text{N}$ -relaxation data including  $T_1$ ,  $T_2$  and  $\{^1\text{H}\}$ - $^{15}\text{N}$  NOE for Rheb $\Delta\text{CT}$  in the GDP- and two GTP analogue-bound states, namely Rheb $\Delta\text{CT}$ -GppNHp and Rheb $\Delta\text{CT}$ -GppCp (Fig. 2, Figs S4 and S7, Tables S1–S6 & Results S1).

The average  $^{15}\text{N}$ - $T_1$  values for Rheb $\Delta\text{CT}$ -GDP are  $676 \pm 34$  ms and  $716 \pm 41$  ms for the GppNHp-bound state at 500-MHz field strength and 298 K. The average  $^{15}\text{N}$ - $T_2$  values are  $90 \pm 15$  ms and  $87 \pm 17$  ms and the average  $\{^1\text{H}\}$ - $^{15}\text{N}$  NOE values are  $0.78 \pm 0.10$  and  $0.79 \pm 0.11$  for the GDP- and GppNHp-bound

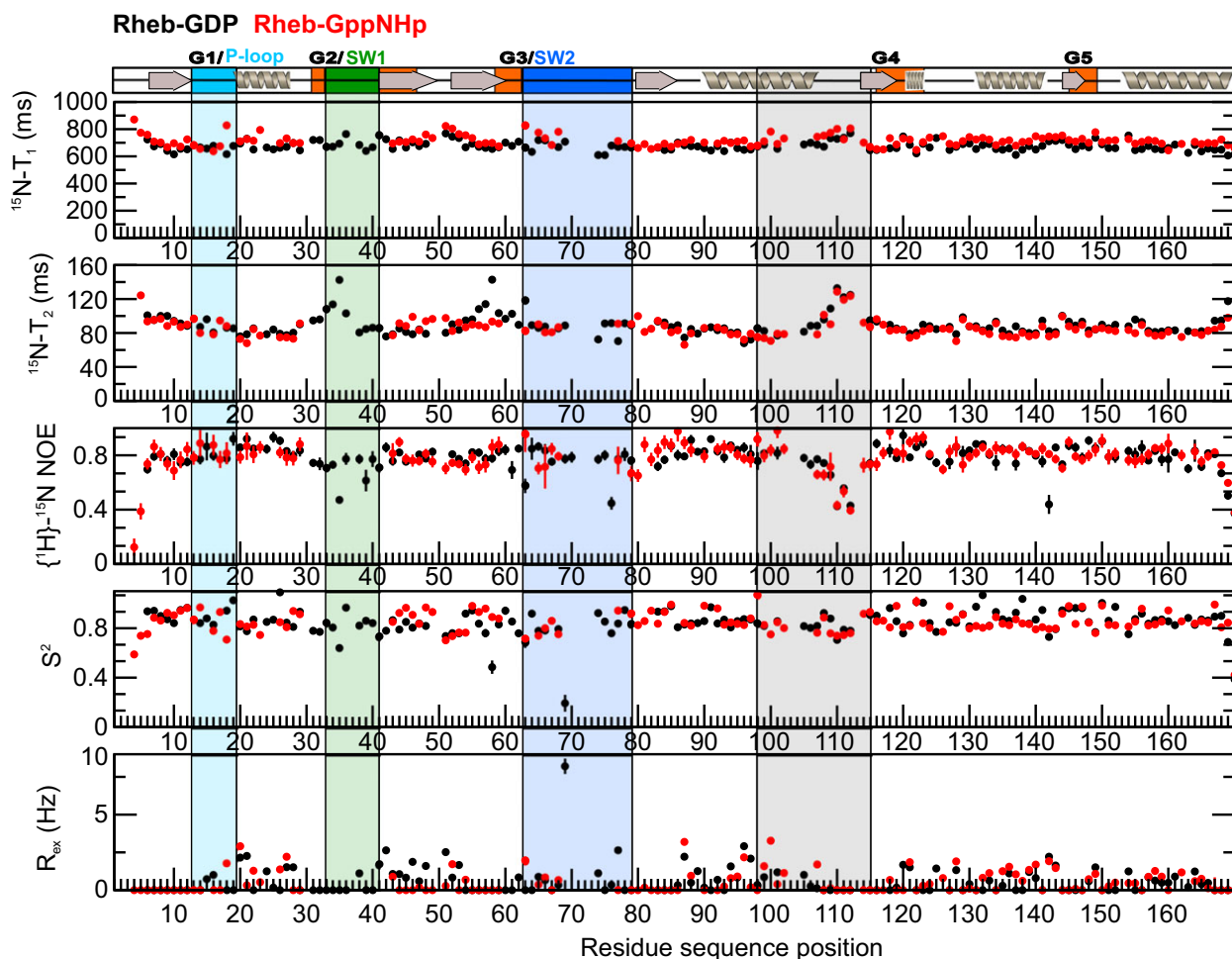


**Fig. 2.** The two switch regions as well as some other residues show increased backbone dynamics. Plots of the  $^{15}\text{N}$ -relaxation data of Rheb $\Delta\text{CT}$  in the GDP- (black) and GppNHp- (red) bound states including  $^{15}\text{N}$ - $T_1$  (top panel),  $^{15}\text{N}$ - $T_2$  (second panel), and  $\{^1\text{H}\}$ - $^{15}\text{N}$  NOE (third panel) values and uncertainties and results of the Lipari-Szabo model-free analysis including the order parameter  $S^2$  (fourth panel) and the contribution of chemical exchange  $R_{\text{ex}}$  to the observed transverse relaxation rate  $1/T_2$  (fifth panel). The model-free analysis of the  $^{15}\text{N}$  relaxation data was performed using the program TENSOR2 [61] and an isotropic tumbling model. The location of the G boxes and the switch 1 and 2 (SW1 & 2) regions [1,3] and the secondary structure elements are indicated at the top. Filled gray arrows represent  $\beta$ -sheet conformation and gray spirals helical conformation. The secondary structure content was derived from the solution structure of C-terminal truncated rat Rheb-GDP (PDB-ID 2L0X) [5]. That of C-terminal truncated mouse Rheb-GppNHp is almost identical (PDB-ID 4O25) [52].

states, respectively. Overall, the  $^{15}\text{N}$ -relaxation parameters are in the range expected for an about 19.3-kDa molecule (GS-human Rheb 1-170). A more extended analysis of the  $^{15}\text{N}$ -relaxation data based on a model-free approach using the program TENSOR2 [61] and an isotropic diffusion tumbling model provides overall rotational correlation times  $\tau_c$  of 9.9 ns for Rheb $\Delta$ CT-GDP and of 10.4 ns for Rheb $\Delta$ CT-GppNHp at 298 K as well as the subnanosecond order parameter  $S^2$  and the parameter  $R_{ex}$ , which contains information about the contribution of conformational exchange to the relaxation process (Fig. 2, bottom two panels, Tables S5 and S6). The fitted  $\tau_c$  values are 1–2 ns lower than estimated based on the number of residues and the molecular weight ( $\approx 11$ –12 ns). This can be explained with the well-defined and compact folds observed for C-terminally truncated rat Rheb-GDP (PDB-ID 2L0X) and mouse Rheb-GppNHp (PDB-ID 4O25) [5,52]. In line with this, most residues show high  $S^2$  order parameter values (Fig. 2, Tables S5 and S6), which are on average  $0.84 \pm 0.15$  and  $0.89 \pm 0.09$  for Rheb $\Delta$ CT-GDP and Rheb $\Delta$ CT-GppNHp, respectively.

Most differences in the backbone dynamics between the inactive GDP- and the active GTP-bound form of Rheb $\Delta$ CT occur in the G2/switch 1 and G3/switch 2 regions (Fig. 2). In the GDP-bound state, Y35 in the switch 1 regions shows higher  $^{15}\text{N}$ - $T_1$  and  $^{15}\text{N}$ - $T_2$  and lower  $\{^1\text{H}\}$ - $^{15}\text{N}$  NOE values, indicating increased backbone dynamics on the ns-ps time scale around this residue. For residues 30–42 of the GppNHp-bound state, no  $^{15}\text{N}$ -relaxation data could be measured since the respective peaks were broadened beyond detection. This suggests that the switch1 region in the GppNHp-bound state shows also increased backbone dynamics, however, on a slightly slower time scale as the GDP-bound state. The same is true for several residues of the G3 box/switch 2 region (63–75) in both states, since residues 70–73 in the GDP and residues 69–76 in the GppNHp-bound state could also not be detected. Differences in the backbone dynamics between Rheb $\Delta$ CT-GDP and Rheb $\Delta$ CT-GppNHp are further observed for residues 18–19 in the P-loop, which are spatially close to the phosphates of the nucleotide and some residues in the subsequent helical region. Finally, for both Rheb $\Delta$ CT-GDP and Rheb $\Delta$ CT-GppNHp residues, G109 to Q112 show higher  $^{15}\text{N}$ - $T_1$  and  $^{15}\text{N}$ - $T_2$  and lower than average  $\{^1\text{H}\}$ - $^{15}\text{N}$  NOE values. Thus, the loop around residues 108–114, which is spatially close to the C-terminal half of the switch 2 region, shows also increased backbone dynamics on the subnanosecond timescale. As expected the dynamic behavior of Rheb $\Delta$ CT in both GTP analogue-bound states (Rheb $\Delta$ CT-GppNHp and Rheb $\Delta$ CT-GppCp) is

overall similar, some differences are seen for residues affected by the type of bound nucleotide (Fig. S4 and Results S1).

### Only Rheb $\Delta$ CT in the active-like GppNHp-bound state weakly interacts with FKBP38-BD

In order to resolve the conflicting results [32,45,46] about the interaction between Rheb and FKBP38 and how far it depends on the nucleotide-binding state of Rheb, NMR-monitored interaction studies were performed. For FKBP38, a protein fragment was used that corresponds to the earlier determined binding domain (BD), which overlaps with the FKBP12-like domain (Fig. 1) [62]. Figure 3A shows the superposition of the  $^1\text{H}$ - $^{15}\text{N}$ HSQC spectra of GDP-bound  $^{15}\text{N}$ -Rheb $\Delta$ CT in the absence and presence of unlabeled FKBP38-BD and in B that of  $^{15}\text{N}$ -FKBP38-BD in the absence and presence of unlabeled Rheb $\Delta$ CT-GDP. Fig. S5C shows further the titration of  $^{15}\text{N}$ -FKBP38-BD with unlabeled Rheb $\Delta$ CT-GDP up to a molar ratio of 1 : 2. In all cases, no significant spectral changes can be observed, indicating that Rheb $\Delta$ CT-GDP does apparently not interact with FKBP38-BD.  $^{15}\text{N}$ -Rheb-GppNHp in the presence of unlabeled FKBP38-BD (Fig. 3C) shows, consistent with the literature suggesting a GTP-dependent interaction [32,62], spectral changes for several residues. Mapping these onto the crystal structure of mouse Rheb-GppNHp (PDB-ID 4O25) [52] (Fig. 3E and Fig. S5A) indicates that the presence of FKBP38-BD affects the long helix containing K97-D105, the nearby W141 and the subsequent loop encompassing residues 108–114. These regions are spatially close to the switch 2 region and based on the  $^{15}\text{N}$ -relaxation data show increased backbone dynamics (Fig. 2). In addition, several residues in the  $\beta$ -sheet region facing the switch 2 region on the other side show medium to weak shifts (e.g. R7, K45, I47, and H55-Q57, respectively). For the part of the switch 2 region that is localized between the mentioned regions, chemical shift changes could mostly not be observed since the backbone amide resonances for residues 69–76 were broadened beyond detection. The chemical shift changes observed in the about 1 : 1 sample of  $^{15}\text{N}$ -Rheb $\Delta$ CT-GppNHp and FKBP38-BD are overall reproduced in the additionally performed titration of  $^{15}\text{N}$ -Rheb $\Delta$ CT-GppNHp with unlabeled FKBP38-BD up to a molar ratio of about 1 : 2 (Fig. S5B). That the  $^1\text{H}$ - $^{15}\text{N}$ -HSQC spectrum of  $^{15}\text{N}$ -FKBP38-BD in the presence of unlabeled Rheb $\Delta$ CT-GppNHp (Fig. 3D) or different concentrations of Rheb $\Delta$ CT-GppCp (Fig. S5D) shows no significant spectral changes may be explained by the interaction



being only weak and/or by the fact that the regions of FKBP38-BD mediating it do not significantly alter their conformation. Addition of unlabeled FKBP38-BD to  $^{15}\text{N}$ -Rheb $\Delta$ CT-GppCp resulted only in a decrease of the GDP state signals that were still present due to a yet incomplete exchange (Fig. S5F, see also next section). Since it had been proposed in the literature that the switch1 region of Rheb plays an important role for the interaction with FKBP38 [62], we further titrated  $^{15}\text{N}$ -FKBP38-BD with a 13mer peptide encompassing the switch 1 region (Fig. S5E). In agreement with the data using Rheb $\Delta$ CT-GDP and Rheb $\Delta$ CT-GppNHp, no significant spectral changes could be observed.

FKBP38 has been shown to contain a low-affinity  $\text{Ca}^{2+}$ -binding site around residues L90-I96 corresponding to residues L147-I153 in the full-length sequence, which modulates the interaction with Bcl-2 [35]. Because of this, we additionally analyzed if FKBP38-BD in the presence of  $\text{CaCl}_2$  interacts stronger with Rheb $\Delta$ CT-GppNHp (Fig. S6). In agreement with published data [35], addition of  $\text{CaCl}_2$  results in very weak shifts for two residues of FKBP38 involved in  $\text{Ca}^{2+}$  binding (C93 and D94, corresponding to C150 and D151 in the full-length sequence) (Fig. S6A). However,  $\text{Ca}^{2+}$  binding to FKBP38-BD appears not to have a significant effect on the affinity for Rheb $\Delta$ CT-GppNHp or vice versa (Fig. S6B,C). Compared with the observed chemical shift changes for  $^{15}\text{N}$ -Rheb $\Delta$ CT-GppNHp in the presence of FKBP38-BD without  $\text{Ca}^{2+}$  (Fig. 3C), those in the presence of  $\text{CaCl}_2$  are similar for the side chain amide of W141 and the backbone amides of the nearby helical residues K97-G101, but the backbone amide cross-peaks of R7, K45, H55-Q57, L83, D105, K109-I112, and A167 showed no significant spectral changes (Fig. S6C). This may at least in part be explained by the fact that the molar ratio of Rheb $\Delta$ CT to FKBP38-BD was lower, only 1 : 0.82 compared to about 1 : 1 in the absence of  $\text{CaCl}_2$ , and that the presence of  $\text{CaCl}_2$  might even have weakened the interaction with the  $\beta$ -sheet region and the loop region around K109-I112. In three independent interaction experiments (Fig. 3C, Figs S5B and S6C) between  $^{15}\text{N}$ -Rheb-GppNHp and FKBP38-BD, the amide cross-peaks of K97 to G101 of the helix next to the switch 2 region and of the nearby W141 (Fig. 3E, Fig. S5A) were consistently showing chemical shift changes. Thus, this region of Rheb appears to be the major interaction side for the GTP-dependent interaction with FKBP38-BD. In line with the above suggestion that this interaction may only be weak, the presence of FKBP38-BD lowered the average  $^{15}\text{N}$ - $T_2$  values of  $^{15}\text{N}$ -Rheb $\Delta$ CT-

GppNHp only slightly from  $87 \pm 17$  ms to  $81 \pm 24$  ms. Moreover, the average  $^{15}\text{N}$ - $T_1$  and  $\{^1\text{H}\}$ - $^{15}\text{N}$  NOE values got also only weakly modulated from  $716 \pm 41$  ms and  $0.79 \pm 0.12$ , respectively, in the absence to  $704 \pm 52$  ms and  $0.79 \pm 0.11$ , respectively, in the presence of FKBP38-BD (Fig. S7, Tables S2 and S4). K97 that shows consistently strong chemical shift changes in  $^{15}\text{N}$ -Rheb $\Delta$ CT-GppNHp in the presence of FKBP38-BD (Fig. 3C, Figs S5B and S6C) shows further a very strong decrease in its  $^{15}\text{N}$ - $T_2$  time from 79 to 30 ms (Tables S2 and S4).

**Weak interactions of the proposed Rheb-binding domain of FKBP38 with the GppNHp- but not the GDP-bound state accelerate the GDP to GTP exchange markedly, but only if FKBP38 is present at a molar ratio to Rheb of 1 : 30 or more**

Guanine nucleotide exchange factors (Fig. 1) typically form ternary complexes with the GDP-bound state in which the GEF is bound loosely and shows the highest affinity for the nucleotide-free state. The affinity for the GTP-bound state is in principle similarly low to that for the GDP-bound one [63,64]. Because the interaction between Rheb $\Delta$ CT-GppNHp and FKBP38-BD is only weak and may be even weaker and thus not detectable for Rheb $\Delta$ CT-GDP, a real-time NMR study was performed (Fig. 4, Figs S8–S10, Table 1) to evaluate if FKBP38 may stimulate the exchange of GDP bound to Rheb $\Delta$ CT for GppNHp. Fig. 4 and Figs S8–S10 show superpositions of the  $^1\text{H}$ - $^{15}\text{N}$  HSQC spectra of  $^{15}\text{N}$ -Rheb $\Delta$ CT-GDP (about 100  $\mu\text{M}$ ) at different time points after adding GppNHp (0.5 mM) in the absence or presence of unlabeled FKBP38-BD at different molar ratios and/or Antarctic phosphatase (= PPase, 5 U) and with 1 or 10 mM EDTA in the buffer. If FKBP38-BD is a GEF (guanine nucleotide exchange factor), the rates for the exchange from GDP to GppNHp should be significantly increased in the presence of low catalytic amounts. For ratios of  $^{15}\text{N}$ -Rheb $\Delta$ CT-GDP to FKBP38-BD of 1 : 102 (series A3, B3, C3, Fig. S8C,F and S9C) or 1 : 96 (series F3, Fig. S9F), the fitted exchange times  $\tau_{\text{ex}}$  (Table 1, Fig. S10C–F) were overall similar or lower than that in the presence of only PPase (series A1, B1, C1, and F1, Fig. S8A,D and S9A, D). If both FKBP38-BD and PPase were present (series A2, B2, C2, and F2, Fig. 4A, Figs S8B,E and S9B,E), the exchange times were higher than with only FKBP38-BD or PPase present in the A2 and B2 series but lower than with PPase alone in the C2 and F2 series (Table 1, Fig. S10C–F). Overall, the exchange time in series A1-3, B1-3, C1-3, and F1-3 was of comparable magnitude (Table 1).

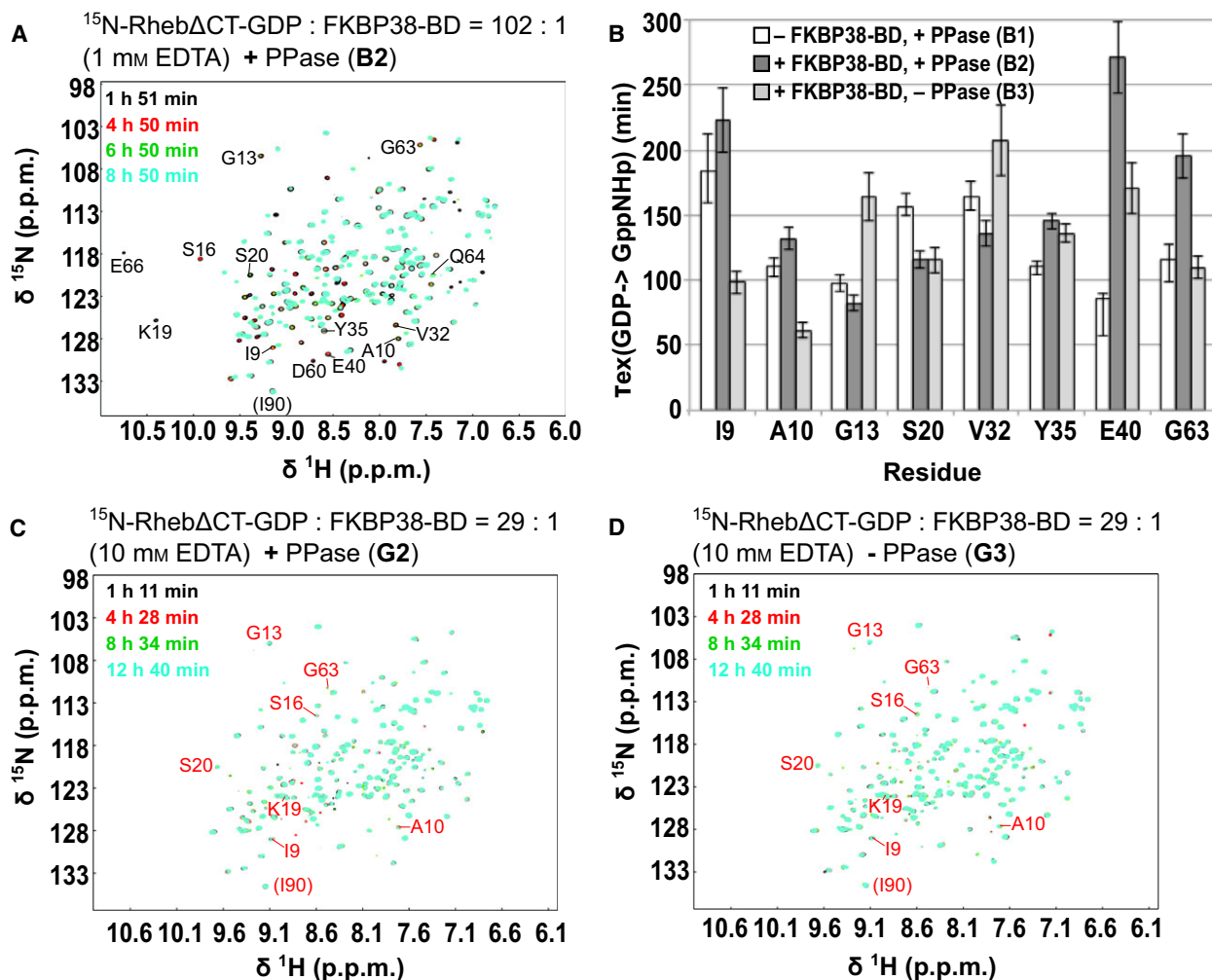


**Fig. 4.** The presence of FKBP38-BD stimulates the GDP to GppNHp exchange of Rheb $\Delta$ CT only weakly if present at low concentrations but significantly if present at higher concentrations. (A) Superposition of the  $^1\text{H}$ - $^{15}\text{N}$  HSQC spectra of  $^{15}\text{N}$ -Rheb $\Delta$ CT-GDP in the presence of GppNHp and unlabeled FKBP38-BD at a molar rate of 1 : 102 as well as catalytic amounts of Antarctic phosphatase (= PPase) after different incubation times. The color coding is indicated in the upper left of the plot. The  $^1\text{H}$ - $^{15}\text{N}$  cross-peaks of the residues of Rheb $\Delta$ CT-GDP showing strong chemical shift changes to the GppNHp-bound state and that have been considered for the rate analysis are labeled with the one letter amino acid code and the residue number. The corresponding analysis for this subseries (**B2** – FKBP38-BD and PPase present) together with that for the other two subseries of this series (**B1** – only PPase, and **B3** – only FKBP38-BD present) are displayed as a function of the residue in (B). Please, see also Table 1, which lists the conditions used for each series together with the average values of the exchange times. (C–D) Superposition of the  $^1\text{H}$ - $^{15}\text{N}$  HSQC spectra of  $^{15}\text{N}$ -Rheb $\Delta$ CT-GDP in the presence of GppNHp and unlabeled FKBP38-BD at a molar rate of 1 : 29 and either catalytic amounts of PPase (C) or no PPase (D) after different incubation times (see upper left of the plot). If FKBP38-BD is present at larger amounts, the exchange is so fast that the peaks of the starting GDP-bound state are mostly not visible anymore. Thus, the peaks of the target GppNHp and not of the starting GDP state have been labeled with the one letter amino acid code and the sequence position.

Thus, at a molar rate of about 1 : 100 of FKBP38-BD to Rheb $\Delta$ CT-GDP, the presence of FKBP38-BD did not strongly accelerate the GDP to GTP exchange. At molar ratios of 1 : 29 (series G2-G3, Fig. 4C,D) or 1 : 15 (series H2-H3, Fig. S10A,B) of  $^{15}\text{N}$ -Rheb $\Delta$ CT-GDP to FKBP38-BD, the exchange of GDP to GppNHp was significantly faster and the spectrum of

the first time point looked already almost like the one of the final fully GppNHp-bound state of Rheb $\Delta$ CT. Because the affinities of the binary complexes between the GTPase and either the nucleotide or its GEF are very high [64], we further prepared a mutant of Rheb $\Delta$ CT (D60K) that cannot interact with nucleotides by site-directed mutagenesis [14]. Presumably due

to the high expression rates in *E. coli*, all the protein was present in inclusion bodies and we did not succeed refolding it (data not shown) and thus were not able to test its interaction with FKBP38-BD.

## Discussion

### The role of increased backbone dynamics in the two switch regions and around residues 98–115 in the inactive GDP- and the active-like GppNHp-bound state of Rheb for the interaction with regulators and effectors

The switch 1 region has generally a critical role in the on- and off-switching cycle of GTPases and for the interaction with other proteins [1,2]. In line with this, the switch 1 region and especially Y35 showed increased backbone dynamics on the ps-ns time scale in Rheb-GDP. The broadening of the peaks for Y35 and the surrounding residues in the GppNHp-bound state indicates also increased backbone dynamics in this state (Fig. 2). Increased mobility around Y32 of Ras (p21<sup>ras</sup>), corresponding to Y35 of Rheb (Fig. S11), was first indicated by <sup>31</sup>P-NMR and EPR data of wild type and mutant proteins and assigned to an interplay with the terminal phosphate groups ( $\beta$ ,  $\gamma$ ) of the bound nucleotide [65]. This observation led to the detection of at least two conformational states of GTP- and GTP analogue-bound Ras [51,65–67]. For the small GTPase Cdc42, it has been shown that replacement of T35, corresponding to T38 in Rheb (Fig. S11), with alanine reduces the conformational freedom and thereby the affinity for a regulatory protein inhibiting GTP hydrolysis [68]. With respect to Rheb, it has been suggested that the switch 1 region plays an important role for the interaction with FKBP38 [62]. However, based on our interaction data (Fig. 3, Figs S5 and S6), the switch 1 region may only indirectly influence the interaction with FKBP38-BD, which is discussed in more detail below. Whereas the switch 1 region shows higher B-factors in the crystal structures of Rheb-GDP and Rheb-GppNHp (55 versus 28.1 and 50 versus 31.1 Å<sup>2</sup> for the whole protein), the switch 2 region shows only somewhat higher B-factors in the GDP- and GppNHp-bound states compared with the whole protein (38.8 versus 28.1 and 35.0 versus 31.1 Å<sup>2</sup>) [4]. Since a few residues of the G3 box/switch 2 region (63–75, Fig. 1A) could not be detected in the GDP- (70–73) and a larger number in the GppNHp-bound (69–76) state (Fig. 2), the switch 2 region shows as the switch 1 region increased backbone dynamics in both nucleotide-binding states (Fig. 2). However, the type of bound nucleotide

modulates the dynamic behavior (Fig. 2, Fig. S4, Tables S1–S6). A similar broadening of NMR signals of the switch 1 and 2 regions in the GppNHp-bound state compared with the GDP-bound state has also been observed for Ras [69]. Regarding this and the overall dynamic properties, our <sup>15</sup>N-relaxation data including besides {<sup>1</sup>H}-<sup>15</sup>N NOE further T<sub>1</sub> and T<sub>2</sub> are in agreement with earlier published {<sup>1</sup>H}-<sup>15</sup>N NOE data for rat Rheb (1–184)-GDP and -GppNHp that differs within 1–170 only at positions 1 and 170 (S1 and I170 compared with M1 and M170 in human Rheb) [5]. The importance of increased backbone dynamics around G63 in the G3 box may explain the finding that replacement of glycine 63 to alanine makes Rheb a more potent mTORC1 activator [52]. In addition, it had already earlier been suggested that the switch 2 region of Rheb is critical for signaling to mTORC1 [70]. Besides the G2 box/switch 1 and the G3 box/switch 2 regions, the region around residues 97–115, which is overall spatially close to the G3/switch 2 region (Fig. 3E), shows similarly increased backbone dynamics in all states of Rheb. A functional role of the region around residues 97–115 is in line with the interaction data for <sup>15</sup>N-Rheb $\Delta$ CT-GppNHp and FKBP38-BD and the <sup>15</sup>N-relaxation data of Rheb $\Delta$ CT-GppNHp in the presence of FKBP38-BD (Fig. S7). Together these indicate that residues 97–101 together with W141 represent the major interaction side of FKBP38-BD on Rheb $\Delta$ CT-GppNHp (Fig. 3, Figs S5 and S6). Interestingly, Rheb-GDP and Rheb-GppNHp tethered to protein–lipid nanodiscs showed increased backbone dynamics for residues in and around the switch regions as well as around residues 90–115 [71]. The increased dynamics of the switch but also the other mentioned regions are expected to facilitate or even enable the interaction with various regulatory proteins [2].

### The Rheb effector FKBP38 accelerates the GDP to GTP exchange by interacting weakly with the active but apparently not the inactive state and may further play a role for membrane targeting

In line with the suggestion that the interaction between Rheb and FKBP38 is GTP-dependent [32], we observed chemical shifts changes for several residues in regions spatially close to the in part undetectable switch 2 region of <sup>15</sup>N-Rheb $\Delta$ CT in the GppNHp-bound state (Fig. 3C,E, Figs S5A,B and S6C) but not the GDP-bound state (Fig. 3A). Since the spectrum of <sup>15</sup>N-FKBP38-BD in the presence of Rheb-GppNHp (Fig. 3D) showed, however, no significant spectral changes, the interaction appears to be only weak or

transient and has only an effect on the structure and dynamics of Rheb $\Delta$ ACT but not FKBP38-BD. Moreover, the chemical shifts changes of Rheb $\Delta$ ACT-GppNHp in the presence of FKBP38-BD become only clearly visible once the GDP to GTP analogue exchange is complete (Fig. 3, Figs S5B and S6C). These two observations and the only weak spectral changes of Rheb $\Delta$ ACT-GppNHp in the presence of FKBP38-BD, which nevertheless have been largely reproduced using three different samples (Fig. 3C,E, Figs S5A,B and S6C), may also explain why one group could not verify this interaction [46], which, however, had been observed by other groups albeit Wang *et al.* mentioned that it must not necessarily be direct [32,45,62]. Discrepancies between the different interaction studies may further be accounted for by differences in the used protein preparation and experimental protocols [32,45,46] and regarding the fact whether Rheb is present in farnesylated form and thus able to localize to membranes or not (see also below) and if other cellular proteins may stabilize the interaction in the pull-downs. It has been proposed that the switch 1 region of Rheb is critical for the interaction with FKBP38 [62]. The presented interaction data between Rheb $\Delta$ ACT and FKBP38-BD (Fig. 3, Figs S5 and S6) including a titration of  $^{15}$ N-FKBP38-BD with a 13mer Rheb switch 1 peptide (Fig. S5E) indicated no chemical shift changes for the switch 1 region if looking at  $^{15}$ N-Rheb or of  $^{15}$ N-FKBP38 in the presence of Rheb $\Delta$ ACT or only the respective switch 1 peptide. Thus, this may be an indirect effect, which reflects the role of the switch I region for the nucleotide binding.

The three main small GTPase-interacting and GTPase-regulatory proteins are GTPase-activating proteins (GAPs) that stimulate GTP hydrolysis and thus deactivation, guanine nucleotide exchange factors (GEFs) that facilitate GDP dissociation and thus activation, and nucleotide dissociation inhibitors (GDI) that regulate the membrane/cytosol alternation [2,63,64]. A GAP for Rheb has been described, namely the TSC complex [15,22]. Since the function of translationally controlled tumor protein (TCTP) as a Rheb GEF [23] has been questioned [24], proteins acting as GEF or GDI for Rheb have still to be found. Because it has already been shown that FKBP38 acts not as GDI for Rheb [46], another aim of this study was to evaluate if FKBP38 might have a GEF-like or another effector effect on Rheb. The presented real-time NMR rate analysis data indicated that the presence of FKBP38-BD in a range more typical for a catalytically acting protein ([Rheb $\Delta$ ACT]:[FKBP38-BD] =  $\approx$  100 : 1) did not strongly accelerate the exchange of GDP to GppNHp (Fig. 4A,B, Table 1, Figs S8 and S9, S10C–

F). However, at molar ratios of Rheb-GDP to FKBP38-BD of 29 : 1 or 15 : 1, FKBP38-BD this was the case (Fig. 4C,D, Fig. S10A,B). For the following reasons, FKBP38 is, however, most likely not a GEF. First, usually low catalytic amounts of GEFs accelerate the GDP to GTP exchange much faster than observed for FKBP38. In a real-time NMR study analyzing the effect of a Rho GEF, it stimulated the exchange about 200-fold if only present at a molar ratio of 1 : 8000 with respect to Rho [72]. Second, GEFs form initially a low-affinity ternary complex with the GDP-bound GTPase, where the nucleotide is still bound tightly. Following a conformational change, the interaction with the nucleotide is weakened and the ternary complex converts into a high-affinity nucleotide-free binary complex. Following binding of GTP, the GEF is released [2,63,64]. In principle, a GEF could also catalyze the reverse reaction, which in the cell does not happen because of the higher concentration of GTP compared with GDP [63]. However, FKBP38-BD appears to have only a weak affinity for the GTP-bound but no significant or if only a very low, in our NMR titrations not detectable, affinity for the GDP-bound form of Rheb (Fig. 3, Figs S5 and S6). Thus, FKBP38-BD shows rather properties typical for a GTPase effector [73], and its apparent GEF-like activity arises because it interacts more favorably with the GppNHp-bound than with the GDP-bound state, thereby driving the equilibrium of the exchange reaction toward the GppNHp-bound state. This happens the faster the more FKBP38-BD is present relative to Rheb-GDP at constant GppNHp concentrations (Table 1). Finally, the known GEFs for Ras family members typically contain a Cdc25-homology catalytic domain [2], which is not the case for FKBP38.

Rheb localizes by a C-terminal farnesyl modification to endomembranes and FKBP38 by a transmembrane domain to the outer mitochondrial membrane [26,41]. Based on NMR studies of Rheb tethered to protein-lipid nanodiscs, it has been shown that the GTPase domain interacts transiently with the bilayer surface with two distinct preferred orientations, which are determined by the bound nucleotide. Moreover, membrane conjugation markedly reduced the rate of intrinsic nucleotide exchange, while GTP hydrolysis was unchanged [71]. Thus, membrane association of Rheb but also of FKBP38 may enhance their interaction and maybe also the newly detected accelerating effect of FKBP38 on the Rheb GDP to GTP exchange. This suggestion would be in line with the observation that the Rheb mutant C181S, which cannot be farnesylated and thus not localize to endomembranes, does not

interact with FKBP38 [45]. Whether FKBP38 is just an effector regulating membrane targeting or shows a more typical GEF-like activity if both Rheb and FKBP38 are membrane bound and present as full-length proteins may be clarified in future studies by a suitable kinetic analysis. In addition, the interaction between Rheb and FKBP38 may be stabilized by the presence of other proteins, which may also be membrane localized, such as components of the mTORC1 complex including TOR itself at the lysosomal membrane or the enzyme phospholipase D1 [74–76]. The proposed low-affinity  $\text{Ca}^{2+}$ -binding site in FKBP38-BD [35] had no significant influence on the interaction with Rheb; however, to date, it has not been analyzed if binding of calmodulin may affect the interaction of FKBP38 with Rheb similarly as that with the apoptosis regulator protein Bcl-2 [39]. Therefore, the role of membrane tethering, other proteins, as well as phosphorylation at S130 of Rheb [77] on the Rheb-FKBP38 interaction, which plays not only a role for mTORC1 signaling [74–76] but also for the regulation of apoptosis [78], should be targeted in more detail within future studies.

## Acknowledgements

This work was supported from the German Research Foundation (DFG grant DA1195/3-1 & 3-2 to SAD). SAD acknowledges further financial support from the TUM diversity and talent management office and the Helmholtz portfolio theme ‘metabolic dysfunction and common disease’ of the Helmholtz Zentrum München. We thank the group of Prof. Dr. Alfred Wittinghofer from the Max-Planck Institute for Molecular Physiology in Dortmund, Germany, for providing an expression plasmid for Rheb $\Delta$ CT; and Prof. Dr. Ho Sup Yoon from the Nanyang Technological University, Singapore, for providing an expression plasmid for FKBP38-BD. We thank Dr. Diana C. Rodriguez Carmargo for purifying some of the used FKBP38-BD protein. We thank Jonas Huber, Eva Lederer, Max Mühlbauer, and Sandra Poser for their contributions while they were doing practical and/or a thesis project in our group. We thank Prof. Dr. Michael Sattler and Prof. Dr. Bernd Reif from the TU München and the Helmholtz Zentrum München very much for hosting our group and for continuous support as well as for sharing their facilities with us.

## Author contributions

SAD designed and coordinated the study, helped acquiring and analyzing the NMR data, and wrote

most of the manuscript. MDC purified the majority of the used protein material, prepared all the samples, recorded and analyzed the NMR data, and helped writing the manuscript. LK analyzed part of the  $^{15}\text{N}$ -relaxation and exchange rate data and helped writing the manuscript. All authors reviewed the results and approved the final version of the manuscript.

## References

- 1 Wittinghofer A and Vetter IR (2011) Structure-function relationships of the G domain, a canonical switch motif. *Annu Rev Biochem* **80**, 943–971.
- 2 Cherfils J and Zeghouf M (2013) Regulation of small GTPases by GEFs, GAPs, and GDIs. *Physiol Rev* **93**, 269–309.
- 3 Heard JJ, Fong V, Bathaie SZ and Tamanoi F (2014) Recent progress in the study of the Rheb family GTPases. *Cell Signal* **26**, 1950–1957.
- 4 Yu Y, Li S, Xu X, Li Y, Guan K, Arnold E and Ding J (2005) Structural basis for the unique biological function of small GTPase RHEB. *J Biol Chem* **280**, 17093–17100.
- 5 Karassek S, Berghaus C, Schwarten M, Goemans CG, Ohse N, Kock G, Jockers K, Neumann S, Gottfried S, Herrmann C *et al.* (2010) Ras homolog enriched in brain (Rheb) enhances apoptotic signaling. *J Biol Chem* **285**, 33979–33991.
- 6 Garami A, Zwartkruis FJ, Nobukuni T, Joaquin M, Rocco M, Stocker H, Kozma SC, Hafen E, Bos JL and Thomas G (2003) Insulin activation of Rheb, a mediator of mTOR/S6K/4E-BP signaling, is inhibited by TSC1 and 2. *Mol Cell* **11**, 1457–1466.
- 7 Inoki K, Li Y, Xu T and Guan KL (2003) Rheb GTPase is a direct target of TSC2 GAP activity and regulates mTOR signaling. *Genes Dev* **17**, 1829–1834.
- 8 Stocker H, Radimerski T, Schindelholz B, Wittwer F, Belawat P, Daram P, Breuer S, Thomas G and Hafen E (2003) Rheb is an essential regulator of S6K in controlling cell growth in *Drosophila*. *Nat Cell Biol* **5**, 559–565.
- 9 Saucedo LJ, Gao X, Chiarelli DA, Li L, Pan D and Edgar BA (2003) Rheb promotes cell growth as a component of the insulin/TOR signalling network. *Nat Cell Biol* **5**, 566–571.
- 10 Hall MN (2016) TOR and paradigm change: cell growth is controlled. *Mol Biol Cell* **27**, 2804–2806.
- 11 Loewith R, Jacinto E, Wullschlegel S, Lorberg A, Crespo JL, Bonenfant D, Oppliger W, Jenoe P and Hall MN (2002) Two TOR complexes, only one of which is rapamycin sensitive, have distinct roles in cell growth control. *Mol Cell* **10**, 457–468.
- 12 Sarbassov DD, Ali SM, Sengupta S, Sheen JH, Hsu PP, Bagley AF, Markhard AL and Sabatini DM (2006)

- Prolonged rapamycin treatment inhibits mTORC2 assembly and Akt/PKB. *Mol Cell* **22**, 159–168.
- 13 Long X, Lin Y, Ortiz-Vega S, Yonezawa K and Avruch J (2005) Rheb binds and regulates the mTOR kinase. *Curr Biol* **15**, 702–713.
- 14 Tabancay AP Jr, Gau CL, Machado IM, Uhlmann EJ, Gutmann DH, Guo L and Tamanoi F (2003) Identification of dominant negative mutants of Rheb GTPase and their use to implicate the involvement of human Rheb in the activation of p70S6K. *J Biol Chem* **278**, 39921–39930.
- 15 Li Y, Inoki K and Guan KL (2004) Biochemical and functional characterizations of small GTPase Rheb and TSC2 GAP activity. *Mol Cell Biol* **24**, 7965–7975.
- 16 Smith EM, Finn SG, Tee AR, Browne GJ and Proud CG (2005) The tuberous sclerosis protein TSC2 is not required for the regulation of the mammalian target of rapamycin by amino acids and certain cellular stresses. *J Biol Chem* **280**, 18717–18727.
- 17 Plank TL, Yeung RS and Henske EP (1998) Hamartin, the product of the tuberous sclerosis 1 (TSC1) gene, interacts with tuberin and appears to be localized to cytoplasmic vesicles. *Cancer Res* **58**, 4766–4770.
- 18 van Slegtenhorst M, Nellist M, Nagelkerken B, Cheadle J, Snell R, van den Ouweland A, Reuser A, Sampson J, Halley D and van der Sluijs P (1998) Interaction between hamartin and tuberin, the TSC1 and TSC2 gene products. *Hum Mol Genet* **7**, 1053–1057.
- 19 Dibble CC, Elis W, Menon S, Qin W, Klekota J, Asara JM, Finan PM, Kwiatkowski DJ, Murphy LO and Manning BD (2012) TBC1D7 is a third subunit of the TSC1-TSC2 complex upstream of mTORC1. *Mol Cell* **47**, 535–546.
- 20 Li Y, Corradetti MN, Inoki K and Guan KL (2004) TSC2: filling the GAP in the mTOR signaling pathway. *Trends Biochem Sci* **29**, 32–38.
- 21 Long X, Ortiz-Vega S, Lin Y and Avruch J (2005) Rheb binding to mammalian target of rapamycin (mTOR) is regulated by amino acid sufficiency. *J Biol Chem* **280**, 23433–23436.
- 22 Zhang Y, Gao X, Saucedo LJ, Ru B, Edgar BA and Pan D (2003) Rheb is a direct target of the tuberous sclerosis tumour suppressor proteins. *Nat Cell Biol* **5**, 578–581.
- 23 Hsu YC, Chern JJ, Cai Y, Liu M and Choi KW (2007) Drosophila TCTP is essential for growth and proliferation through regulation of dRheb GTPase. *Nature* **445**, 785–788.
- 24 Rehmann H, Brüning M, Berghaus C, Schwarten M, Köhler K, Stocker H, Stoll R, Zwartkruis FJ and Wittinghofer A (2008) Biochemical characterisation of TCTP questions its function as a guanine nucleotide exchange factor for Rheb. *FEBS Lett* **582**, 3005–3010.
- 25 Tee AR, Blenis J and Proud CG (2005) Analysis of mTOR signaling by the small G-proteins, Rheb and RhebL1. *FEBS Lett* **579**, 4763–4768.
- 26 Buerger C, DeVries B and Stambolic V (2006) Localization of Rheb to the endomembrane is critical for its signaling function. *Biochem Biophys Res Commun* **344**, 869–880.
- 27 Hanker AB, Mitin N, Wilder RS, Henske EP, Tamanoi F, Cox AD and Der CJ (2010) Differential requirement of CAAX-mediated posttranslational processing for Rheb localization and signaling. *Oncogene* **29**, 380–391.
- 28 De Cicco M, Rahim MS and Dames SA (2015) Regulation of the target of rapamycin and other phosphatidylinositol 3-kinase-related kinases by membrane targeting. *Membranes (Basel)* **5**, 553–575.
- 29 Sancak Y, Bar-Peled L, Zoncu R, Markhard AL, Nada S and Sabatini DM (2010) Ragulator-Rag complex targets mTORC1 to the lysosomal surface and is necessary for its activation by amino acids. *Cell* **141**, 290–303.
- 30 Sancak Y, Peterson TR, Shaul YD, Lindquist RA, Thoreen CC, Bar-Peled L and Sabatini DM (2008) The Rag GTPases bind raptor and mediate amino acid signaling to mTORC1. *Science* **320**, 1496–1501.
- 31 Groenewoud MJ and Zwartkruis FJ (2013) Rheb and Rags come together at the lysosome to activate mTORC1. *Biochem Soc Trans* **41**, 951–955.
- 32 Bai X, Ma D, Liu A, Shen X, Wang QJ, Liu Y and Jiang Y (2007) Rheb activates mTOR by antagonizing its endogenous inhibitor, FKBP38. *Science* **318**, 977–980.
- 33 Dunlop EA, Dodd KM, Seymour LA and Tee AR (2009) Mammalian target of rapamycin complex 1-mediated phosphorylation of eukaryotic initiation factor 4E-binding protein 1 requires multiple protein-protein interactions for substrate recognition. *Cell Signal* **21**, 1073–1084.
- 34 Maestre-Martinez M, Edlich F, Jarczowski F, Weiwad M, Fischer G and Lucke C (2006) Solution structure of the FK506-binding domain of human FKBP38. *J Biomol NMR* **34**, 197–202.
- 35 Maestre-Martinez M, Haupt K, Edlich F, Neumann P, Parthier C, Stubbs MT, Fischer G and Lucke C (2011) A charge-sensitive loop in the FKBP38 catalytic domain modulates Bcl-2 binding. *J Mol Recognit* **24**, 23–34.
- 36 Haupt K, Jahreis G, Linnert M, Maestre-Martinez M, Malesevic M, Pechstein A, Edlich F and Lucke C (2012) The FKBP38 catalytic domain binds to Bcl-2 via a charge-sensitive loop. *J Biol Chem* **287**, 19665–19673.
- 37 Maestre-Martinez M, Haupt K, Edlich F, Jahreis G, Jarczowski F, Erdmann F, Fischer G and Lucke C (2010) New structural aspects of FKBP38 activation. *Biol Chem* **391**, 1157–1167.

- 38 Kang CB, Tai J, Chia J and Yoon HS (2005) The flexible loop of Bcl-2 is required for molecular interaction with immunosuppressant FK-506 binding protein 38 (FKBP38). *FEBS Lett* **579**, 1469–1476.
- 39 Edlich F, Weiwad M, Erdmann F, Fanghanel J, Jarczowski F, Rahfeld JU and Fischer G (2005) Bcl-2 regulator FKBP38 is activated by Ca<sup>2+</sup> /calmodulin. *EMBO J* **24**, 2688–2699.
- 40 Kang C, Ye H, Chia J, Choi BH, Dhe-Paganon S, Simon B, Schütz U, Sattler M and Yoon HS (2013) Functional role of the flexible N-terminal extension of FKBP38 in catalysis. *Sci Rep* **3**, 2985.
- 41 Shirane M and Nakayama KI (2003) Inherent calcineurin inhibitor FKBP38 targets Bcl-2 to mitochondria and inhibits apoptosis. *Nat Cell Biol* **5**, 28–37.
- 42 Wang HQ, Nakaya Y, Du Z, Yamane T, Shirane M, Kudo T, Takeda M, Takebayashi K, Noda Y, Nakayama KI *et al.* (2005) Interaction of presenilins with FKBP38 promotes apoptosis by reducing mitochondrial Bcl-2. *Hum Mol Genet* **14**, 1889–1902.
- 43 Nakagawa T, Shirane M, Iemura S, Natsume T and Nakayama KI (2007) Anchoring of the 26S proteasome to the organellar membrane by FKBP38. *Genes Cells* **12**, 709–719.
- 44 Wang J, Tong W, Zhang X, Chen L, Yi Z, Pan T, Hu Y, Xiang L and Yuan Z (2006) Hepatitis C virus non-structural protein NS5A interacts with FKBP38 and inhibits apoptosis in Huh7 hepatoma cells. *FEBS Lett* **580**, 4392–4400.
- 45 Wang X, Fonseca BD, Tang H, Liu R, Elia A, Clemens MJ, Bommer UA and Proud CG (2008) Re-evaluating the roles of proposed modulators of mammalian target of rapamycin complex 1 (mTORC1) signaling. *J Biol Chem* **283**, 30482–30492.
- 46 Uhlenbrock K, Weiwad M, Wetzker R, Fischer G, Wittinghofer A and Rubio I (2009) Reassessment of the role of FKBP38 in the Rheb/mTORC1 pathway. *FEBS Lett* **583**, 965–970.
- 47 John J, Rensland H, Schlichting I, Vetter I, Borasio GD, Goody RS and Wittinghofer A (1993) Kinetic and structural analysis of the Mg(2+) -binding site of the guanine nucleotide-binding protein p21H-ras. *J Biol Chem* **268**, 923–929.
- 48 Marshall CB, Meiri D, Smith MJ, Mazhab-Jafari MT, Gasmi-Seabrook GM, Rottapel R, Stambolic V and Ikura M (2012) Probing the GTPase cycle with real-time NMR: GAP and GEF activities in cell extracts. *Methods* **57**, 473–485.
- 49 Marshall CB, Ho J, Buerger C, Plevin MJ, Li GY, Li Z, Ikura M and Stambolic V (2009) Characterization of the intrinsic and TSC2-GAP-regulated GTPase activity of Rheb by real-time NMR. *Sci Signal* **2**, ra3.
- 50 John J, Sohmen R, Feuerstein J, Linke R, Wittinghofer A and Goody RS (1990) Kinetics of interaction of nucleotides with nucleotide-free H-ras p21. *Biochemistry* **29**, 6058–6065.
- 51 Spoerner M, Nuehs A, Ganser P, Herrmann C, Wittinghofer A and Kalbitzer HR (2005) Conformational states of Ras complexed with the GTP analogue GppNHp or GppCH2p: implications for the interaction with effector proteins. *Biochemistry* **44**, 2225–2236.
- 52 Mazhab-Jafari MT, Marshall CB, Ho J, Ishiyama N, Stambolic V and Ikura M (2014) Structure-guided mutation of the conserved G3-box glycine in Rheb generates a constitutively activated regulator of mammalian target of rapamycin (mTOR). *J Biol Chem* **289**, 12195–12201.
- 53 Corsello S, Fulgenzi A, Vietti D and Ferrero ME (2009) The usefulness of chelation therapy for the remission of symptoms caused by previous treatment with mercury-containing pharmaceuticals: a case report. *Cases J* **2**, 199.
- 54 Conyers RAJ, Birkett DJ, Neale FC, Posen S and Brudenellwoods J (1967) The action of EDTA on human alkaline phosphatases. *Biochim Biophys Acta* **139**, 363–371.
- 55 Delaglio F, Grzesiek S, Vuister GW, Zhu G, Pfeifer J and Bax A (1995) NMRPipe: a multidimensional spectral processing system based on UNIX pipes. *J Biomol NMR* **6**, 277–293.
- 56 Johnson BA (2004) Using NMRView to visualize and analyze the NMR spectra of macromolecules. *Methods Mol Biol* **278**, 313–352.
- 57 Berghaus C, Schwarten M, Heumann R and Stoll R (2007) Sequence-specific 1H, 13C, and 15N backbone assignment of the GTPase rRheb in its GDP-bound form. *Biomol NMR Assign* **1**, 45–47.
- 58 Schwarten M, Berghaus C, Heumann R and Stoll R (2007) Sequence-specific 1H, 13C, and 15N backbone assignment of the activated 21 kDa GTPase rRheb. *Biomol NMR Assign* **1**, 105–108.
- 59 Mandel AM, Akke M and Palmer AG III (1995) Backbone dynamics of Escherichia coli ribonuclease HI: correlations with structure and function in an active enzyme. *J Mol Biol* **246**, 144–163.
- 60 Lipari G and Szabo A (1982) Model-free approach to the interpretation of nuclear magnetic resonance relaxation in macromolecules. 1. Theory and range of validity. *J Am Chem Soc* **104**, 4546–4559.
- 61 Dosset P, Hus JC, Blackledge M and Marion D (2000) Efficient analysis of macromolecular rotational diffusion from heteronuclear relaxation data. *J Biomol NMR* **16**, 23–28.
- 62 Ma D, Bai X, Guo S and Jiang Y (2008) The switch I region of Rheb is critical for its interaction with FKBP38. *J Biol Chem* **283**, 25963–25970.
- 63 Wittinghofer F (1998) Ras signalling. Caught in the act of the switch-on. *Nature* **394**, 317, 319–20.

- 64 Bos JL, Rehmann H and Wittinghofer A (2007) GEFs and GAPs: critical elements in the control of small G proteins. *Cell* **129**, 865–877.
- 65 Geyer M, Schweins T, Herrmann C, Prisner T, Wittinghofer A and Kalbitzer HR (1996) Conformational transitions in p21ras and in its complexes with the effector protein Raf-RBD and the GTPase activating protein GAP. *Biochemistry* **35**, 10308–10320.
- 66 Spoerner M, Hozsa C, Poetzl JA, Reiss K, Ganser P, Geyer M and Kalbitzer HR (2010) Conformational states of human rat sarcoma (Ras) protein complexed with its natural ligand GTP and their role for effector interaction and GTP hydrolysis. *J Biol Chem* **285**, 39768–39778.
- 67 Long D, Marshall CB, Bouvignies G, Mazhab-Jafari MT, Smith MJ, Ikura M and Kay LE (2013) A comparative CEST NMR study of slow conformational dynamics of small GTPases complexed with GTP and GTP analogues. *Angew Chem Int Ed Engl* **52**, 10771–10774.
- 68 Chandrashekar R, Salem O, Krizova H, McFeeters R and Adams PD (2011) A switch I mutant of Cdc42 exhibits less conformational freedom. *Biochemistry* **50**, 6196–6207.
- 69 Ito Y, Yamasaki K, Iwahara J, Terada T, Kamiya A, Shirouzu M, Muto Y, Kawai G, Yokoyama S, Laue ED *et al.* (1997) Regional polyesterism in the GTP-bound form of the human c-Ha-Ras protein. *Biochemistry* **36**, 9109–9119.
- 70 Long X, Lin Y, Ortiz-Vega S, Busch S and Avruch J (2007) The Rheb switch 2 segment is critical for signaling to target of rapamycin complex 1. *J Biol Chem* **282**, 18542–18551.
- 71 Mazhab-Jafari MT, Marshall CB, Stathopoulos PB, Kobashigawa Y, Stambolic V, Kay LE, Inagaki F and Ikura M (2013) Membrane-dependent modulation of the mTOR activator Rheb: NMR observations of a GTPase tethered to a lipid-bilayer nanodisc. *J Am Chem Soc* **135**, 3367–3370.
- 72 Gasmi-Seabrook GM, Marshall CB, Cheung M, Kim B, Wang F, Jang YJ, Mak TW, Stambolic V and Ikura M (2010) Real-time NMR study of guanine nucleotide exchange and activation of RhoA by PDZ-RhoGEF. *J Biol Chem* **285**, 5137–5145.
- 73 Goody RS and Hofmann-Goody W (2002) Exchange factors, effectors, GAPs and motor proteins: common thermodynamic and kinetic principles for different functions. *Eur Biophys J* **31**, 268–274.
- 74 Dibble CC and Cantley LC (2015) Regulation of mTORC1 by PI3K signaling. *Trends Cell Biol* **25**, 545–555.
- 75 Efeyan A, Zoncu R and Sabatini DM (2012) Amino acids and mTORC1: from lysosomes to disease. *Trends Mol Med* **18**, 524–533.
- 76 Avruch J, Long X, Ortiz-Vega S, Rapley J, Papageorgiou A and Dai N (2009) Amino acid regulation of TOR complex 1. *Am J Physiol Endocrinol Metab* **296**, E592–E602.
- 77 Zheng M, Wang YH, Wu XN, Wu SQ, Lu BJ, Dong MQ, Zhang H, Sun P, Lin SC, Guan KL *et al.* (2011) Inactivation of Rheb by PRAK-mediated phosphorylation is essential for energy-depletion-induced suppression of mTORC1. *Nat Cell Biol* **13**, 263–272.
- 78 Ma D, Bai X, Zou H, Lai Y and Jiang Y (2010) Rheb GTPase controls apoptosis by regulating interaction of FKBP38 with Bcl-2 and Bcl-XL. *J Biol Chem* **285**, 8621–8627.

## Supporting information

Additional Supporting Information may be found online in the supporting information tab for this article:

**Fig. S1.**  $^1\text{H}$ - $^{15}\text{N}$  spectrum of Rheb $\Delta\text{CT}$  in the GDP-bound state.

**Fig. S2.**  $^1\text{H}$ - $^{15}\text{N}$  HSQC spectrum of Rheb $\Delta\text{CT}$  in the GppNHp-bound state.

**Fig. S3.** (A) Superposition of the  $^1\text{H}$ - $^{15}\text{N}$  HSQC spectra of Rheb $\Delta\text{CT}$  in the GppNHp- (red) and GppCp- (green) bound states. (B) Larger  $^1\text{H}$ - $^{15}\text{N}$  HSQC spectrum of Rheb $\Delta\text{CT}$  in the GppCp-bound state.

**Fig. S4.** Comparison of the backbone dynamics of Rheb $\Delta\text{CT}$  in the GppNHp- (red) and GppCp- (green) bound states. Shown are plots of the  $^{15}\text{N}$ -relaxation data including  $^{15}\text{N}$ - $T_1$  (top panel),  $^{15}\text{N}$ - $T_2$  (second panel), and  $\{^1\text{H}\}$ - $^{15}\text{N}$  NOE (third panel) values.

**Fig. S5.** More NMR data recorded to characterize the interaction between Rheb $\Delta\text{CT}$  and FKBP38-BD.

**Fig. S6.** NMR data recorded to characterize a potential influence of the addition of  $\text{CaCl}_2$  on the interaction between FKBP38-BD and Rheb $\Delta\text{CT}$ .

**Fig. S7.** Comparison of the backbone dynamics of Rheb $\Delta\text{CT}$  in the GppNHp-bound state in the absence (red) and presence (blue) of unlabeled FKBP38-BD. Shown are plots of the  $^{15}\text{N}$  relaxation data including  $^{15}\text{N}$ - $T_1$  (top panel),  $^{15}\text{N}$ - $T_2$  (second panel), and  $\{^1\text{H}\}$ - $^{15}\text{N}$  NOE (third panel) values.

**Fig. S8.** More NMR data regarding the effect of FKBP38-BD on the GDP to GppNHp exchange of Rheb $\Delta\text{CT}$ .

**Fig. S9.** More NMR data regarding the effect of FKBP38-BD on the GDP to GppNHp exchange of Rheb $\Delta\text{CT}$ .

**Fig. S10.** Superposition of the  $^1\text{H}$ - $^{15}\text{N}$  HSQC spectra of  $^{15}\text{N}$ -Rheb $\Delta\text{CT}$ -GDP in the presence of GppNHp and unlabeled FKBP38-BD at a molar ratio of 1 : 15 (series H)

and either catalytic amounts of Antarctic phosphatase (= PPase) (A) or no Antarctic phosphatase (B) after different incubation times.

**Fig. S11.** Picture of the alignment of the amino acid sequences of human Rheb, Ras (p21ras), and Cdc42.

**Table S1.**  $^{15}\text{N}$ -relaxation times  $T_1$  and  $T_2$ , and  $\{^1\text{H}\}$ - $^{15}\text{N}$  NOE values and corresponding errors for the GDP-bound form of Rheb $\Delta\text{CT}$ .

**Table S2.**  $^{15}\text{N}$ -relaxation times  $T_1$  and  $T_2$ , and  $\{^1\text{H}\}$ - $^{15}\text{N}$  NOE values and corresponding errors for the GppNHp-bound form of Rheb $\Delta\text{CT}$ .

**Table S3.**  $^{15}\text{N}$ -relaxation times  $T_1$  and  $T_2$ , and  $\{^1\text{H}\}$ - $^{15}\text{N}$  NOE values and corresponding errors for the GppCp-

bound form of Rheb $\Delta\text{CT}$ .

**Table S4.**  $^{15}\text{N}$ -relaxation times  $T_1$  and  $T_2$ , and  $\{^1\text{H}\}$ - $^{15}\text{N}$  NOE values and corresponding errors for the GppNHp-bound form of Rheb $\Delta\text{CT}$  in the presence of FKBP38-BD.

**Table S5.** Results from the Lipari and Szabo model-free analysis of the  $^{15}\text{N}$ -relaxation data of Rheb $\Delta\text{CT}$  bound to GDP with TENSOR2.

**Table S6.** Results from the Lipari and Szabo model-free analysis of the  $^{15}\text{N}$ -relaxation data of Rheb $\Delta\text{CT}$  bound to GppNHp with TENSOR2.

**Results S1.** Comparison of the backbone dynamics of two different GTP analogue-bound states of Rheb $\Delta\text{CT}$ .